Proceedings of the 2nd World Congress on New Technologies (NewTech'16)
Budapest, Hungary – August 18 – 19, 2016
Paper No. ICNFA 152
DOI: 10.11159/icnfa16.152

Exciton and Trion in 2D Transition Metal Dichalcogenides

A. Hichri[1], S. Ayari[1], S. Ben Nasseur[1], S. Jaziri[1, 2]
[1]Département de Physique, Laboratoire de Physique des Matériaux, Faculté des Sciences de Bizerte 7021 Jarzouna, Université de Carthage, Tunisie.
[2]Laboratoire de physique de la matière condensée, Faculté des Sciences de Tunis 2092 El Manar, Université El Manar, Tunisie
aida.ezzeddini@gmail.com; sabrineayari4@yahoo.fr; sirinamarouan@gmail.com; sihem.jaziri@fsb.rnu.tn

Abstract - Two-dimensional (2D) layered transition metal dichalcogenides (TMDs) semiconductors such as MoS_2, $MoSe_2$, WS_2,WSe_2 have established themselves as strong contenders for next-generation electronics and optoelectronics and they have aroused great attention due to their peculiar physical properties, in particular the strong electron-hole interaction. We present a theoretical model based on non-local dielectric screening potential to show the impact of the screening length and the reduced mass on the exciton binding energy. We will also determine the oscillator strength and the photoluminescence (PL) line shape in order to compare between the four TMDs types and to prove that they have a large trion binding energy.

Keywords**:** exciton, trion, binding energy, non-local dielectric screening potential, dielectric screening length, transition metal dichalcogenides(TMDs), two dimensional materials(2D), photoluminescence(PL).

1. Introduction

Thin 2D materials, such as graphene, hexagonal boron-nitride (h-BN) and the TMDs [1] are currently being intensively researched due to their electrical and optical properties and have sparked wide interest in both device physics and technological applications at the atomic monolayer limit. In fact, TMD materials provide what neither graphene nor h-BN can. Therefore, there is hope to integrate these materials for numerous device types for many applications in photonics [2], flexible electronics [2], high performance electronics [2], field effect transistors [3], photo detectors [4], light-emitting diodes (sensors) [5], and solar cells [6]. The TMDs with the chemical formula MX_2,where the transition metal M (Mo, W, Ta, Nb, Zr, Ti) is sandwiched by two chalcogens X (S, Se, Te), present a particularly interesting class of 2D materials comprising semi-conductors (MoS_2, $MoSe_2$, WS_2, WSe_2) with band gap between (1-3eV), semi-metals (WTe_2, $TiSe_2$) with band gap between (0-1eV), metals ($NbTe_2$, $TaTe_2$,NbS_2, VS_2) and superconductors (NbS_2, $NbSe_2$, TaS_2) [7]. In the bulk form, MX_2 compounds are layered materials (or van der Waals solids) in which there is strong intralayer binding and weak interlayer binding. The isolation of monolayer's of TMDs leads to the dramatic changes in their properties, primarily due to the confinement of charge carriers in two dimensions (x- and y-directions) due to the absence of interactions in the z-direction. Thus, single layered nano sheets are two-dimensional materials that possess dramatically different fundamental properties compared to their bulk counterparts. In total, there exist ~60 TMD compounds, 2/3 of which have layered structure and in principle could exist in the 2D form. Moreover, the two most important characteristics of the 2D semiconductors are the circular dichroism in combination with strong spin orbit coupling and the inherent extraordinary strong Coulomb interaction.

Currently, optoelectronic research in monolayer TMDs has concentrated on the molybdenum (Mo) and tungsten (W) based compounds (MoS_2, $MoSe_2$, WS_2, and WSe_2). Their bulk crystals are indirect band gap, and they were shown to undergo a transition to direct band gap materials when their thickness is thinned down to a single layer [8] which shared the same honeycomb hexagonal lattice as graphene. The strong quantum confinement and reduced screening in the strict 2D limit, charge carriers in monolayer TMDs are subject to significant Coulomb interactions. The resulting formation of bound electron-hole pairs or exciton ($X = eh$) can be observable even at room temperature. This large binding energy exciton exhibit behavior similar to excited atoms, with energy levels designated 1s, 2s, 3s….. In addition, exciton can capture an additional charge to form negatively charged exciton known as trion ($X^- = eeh$). The investigation of the trion in TMDs is accomplished by several theoretical and experimental studies such as scanning tunneling spectroscopy, temperature-dependent PL and nonlinear optical spectroscopy. The obtained binding energies of trions are about 15-45meV in monolayer

TMDs [9], for example MoS_2 (20 meV) WSe_2 (30 meV) ,WS_2 (45 meV) ,and those of exciton in monolayer MoS_2, $MoSe_2$,WSe_2 and WS_2 are in a range of 200 to 600 meV [10-12]. Despite TMDs are not directly bonded with the environment due to their thickness, they are highly sensitive to electromagnetic fields, doping, or dielectric screening of their surroundings. Consequently, the Coulomb interaction between an electron and a hole in exciton is screened by the dielectric environment and the binding energy changes considerably [13].

In this work we present a microscopic theory of both excitonic and trionic effects in monolayers TMDs especially MoS_2, $MoSe_2$, WS_2 and WSe_2 . We identify and characterize the ground state exciton and trion using a non-local screening Coulomb potential. We calculate the PL line shape of these four single layer TMDs.

2. Exciton

Optical properties play a central role in 2D TMDs. It is therefore of almost importance to understand the optical mechanism, which has dominated by strong excitonic character. The electron-hole (e-h) pair in theses 2Dsemiconductors are governed by screened Coulomb potential $V_s(\rho) = -\frac{e^2}{\varepsilon_1+\varepsilon_2}\int \frac{q_s dq}{q+q_s} J_0(q\rho)$, with $|\vec{\rho}| = |\vec{r}_e - \vec{r}_h|$, $\vec{r}_e$ and $\vec{r}_h$ are the electron and hole positions respectively, $J_0(q\rho)$ is the Bessel function of the first kind, $\vec{q}$ is the electron's wave vector and q_s is the inverse 2D screening length $r_s = \frac{\epsilon_r d}{\varepsilon_1+\varepsilon_2}$ that depends on the environmental relative dielectric constants ε_1 (vacuum) and ε_2 (substrate) and on the relative dielectric constant of the material ϵ_r where d is the effective width of the TMDs layer. The effective Hamiltonian including the dielectric screening can be written as follow $H_X = \frac{\vec{P}_e^2}{2m_e} + \frac{\vec{P}_h^2}{2m_h} + V_s(\rho)$ whe re $m_{e,h}$ are the effective electron and hole masses, respectively and are given in term of the free electron mass m_0. Using relative- $\vec{\rho}$ and center of mass- coordinate of the exciton $\vec{R}_X = \frac{m_e\vec{r_e}+m_h\vec{r_h}}{m_e+m_h}$, the Hamiltonian becomes $H_X = \frac{\vec{P}^2}{2M_X} + \frac{\vec{p}^2}{2\mu} + V_s(\rho)$. The first term is the center of mass Hamiltonian which has a solution of plane wave $\frac{1}{\sqrt{S}} e^{i\vec{K}\vec{R}_X}$, where $\vec{K}$ which is a good quantum number, represents the exciton's center of mass wave vector, $M_X = m_e + m_h$ is the exciton effective mass and S is the area of the monolayer. The second term refers to the relative exciton Hamiltonian $H_{rel} = \frac{\vec{p}^2}{2\mu} + V_s(\rho)$, $\mu = \frac{m_e m_h}{m_e+m_h}$ is the reduced effective mass in the 2D plan. To solve the eigenvalues equation involving H_{rel}, we used a wave function expansion technique. The solution $\phi_{rel}(\vec{\rho},\theta) = \sum_{n,l} c_{n,l}\zeta_{n,l}(\vec{\rho},\theta)$ is extended in term of the orthogonal Laguerre polynomial $L^{2|l|}_{n-|l|-1}(x)$ (solution of the 2D hydrogenic model $\zeta_{n,l}(\rho,\theta) = \sqrt{\frac{2}{\pi}}\left\{\left[\frac{2}{(2n-1)\delta a_b}\right]^2 \frac{(n-|l|-1)!}{(n+|l|-1)!(2n-1)}\right\}^{\frac{1}{2}} e^{il\theta}\left(\frac{4\rho}{(2n-1)\delta a_b}\right)^{|l|} e^{-\frac{2\rho}{(2n-1)\delta a_b}} L^{2|l|}_{n-|l|-1}\left(\frac{4\rho}{(2n-1)\delta a_b}\right)$, $n \in \mathbb{N}^*$ is a state degenerate with angular momentum l = 0, ±1,…, ± $(n-1)$, with $a_b = \frac{\varepsilon_r\hbar^2}{\mu e^2}$ is the exciton effective Bohr radius, $\delta = \frac{d}{2r_s}$. Using numerical diagonalization we obtain the eigenvalues and eigenfunctions of the exciton solution of the total Hamiltonian expressed as $E^X_{n,l} = E_g + \frac{\hbar^2K^2}{2M_X} + E_{n,l}$ and $\psi_{n,l}(\vec{R}_X,\vec{\rho},\theta) = \frac{1}{\sqrt{S}} e^{i\vec{K}\vec{R}_X}\phi_{rel}(\vec{\rho},\theta)$ where E_g is the band gap. We restrict ourselves to the fundamental state.

We plot in fig.1, the binding energy E^X_b for the exciton ground state as a function of reduced mass and screening length. The parameters of the obtained results are extracted from [14] except for WS_2 [13]. We notice three regions for which the exciton binding energy is significantly decreased. For small dielectric screening length i.e.$r_s < 5{,}5$ Å, exciton binding energy is dramatically decreased with increasing reduced mass. In this area, exciton binding energy can exceed largely the values obtained by the most experiment and theoretical work. For example the binding energies extracted from two-photon excitation studies[15] and reflectivity studies [16] are about 700-830 meV for monolayer WS_2. For $5{,}5$ Å $< r_s < 8$ Å, the energy decreases rapidly from 700 to 150 meV. In comparison with MoS_2, WS_2 has the largest exciton binding energy. In the rest of the spectrum, the exciton binding energy varies slowly as a function of these two parameters.

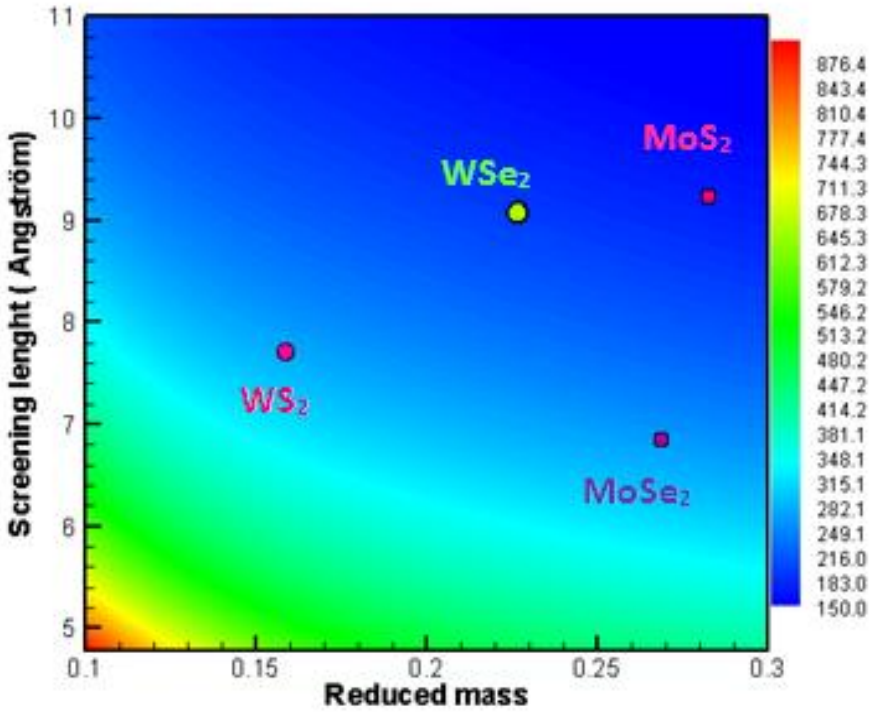

Fig. 1: Plot of the calculated 1s exciton binding energy (meV) using the non-local dielectric screening potential over a range of reduced mass (x m_0) and screening length r_s.

These results highlight a further interesting consequence of the screening potential, which that exciton binding energies scale only weakly and nonlinearly with the reduced mass. Next, we discuss the trion optical spectra.

3. Trion

We adopt the same formalism to investigate the trion binding energy in monolayer TMDs. We start by the trionic Hamiltonian which given by: $H_T = \sum_i H_{Xi} - \frac{1}{2m_h}\vec{\nabla}_{\rho 1}.\vec{\nabla}_{\rho 2} - V_s(\rho_1 - \rho_2)$ where i=1, 2 refer to the first and the second exciton corresponding to the relative coordinates $\vec{\rho}_i = \vec{r}_{ei} - \vec{r}_h$. We use relative $(\vec{\rho}_1, \vec{\rho}_2)$ and center of mass $\vec{R}_T = \frac{M_X\vec{R}_X + m_e\vec{r}_{e2}}{M_T}$ coordinates of the two quasi-particles (exciton 1 and exciton 2) with $M_T = 2m_e + m_h$ is the trion mass. As the in-plane center of mass motion is also separated from the relative motion, and then the trion wave function $\chi_{n,l,n',l'}(\vec{\rho}_1, \vec{\rho}_2, \vec{R}_T)$ can be written as the product of the center of mass contribution and the relative wave function $\zeta_{n,l}(\vec{\rho}_i)$: $\chi_{n,l,n',l'}(\vec{\rho}_1, \vec{\rho}_2, \vec{R}_T) = \frac{1}{\sqrt{S}} e^{-i\vec{Q}\vec{R}_T}\zeta_{n,l}(\vec{\rho}_1) \times \zeta_{n',l'}(\vec{\rho}_2)$ where $\vec{Q}$ is the trion center of mass wave vector. Applying the similar numerical diagonalization we obtained eigenvalues $E^T_{n,l}$ and eigenvectors $\psi_{nT}(\vec{\rho}_1, \vec{\rho}_2, \vec{R}_T)$.

In order to obtain the optical spectrum (PL) line shape, we restrict ourselves to the fundamental exciton and trion states, $P^X(\omega) = |\psi_{1s}(\rho = 0)|^2 \int f_c^X(\vec{K})\delta\left(\hbar\omega - E^X_{1s} - \frac{\hbar^2 K^2}{2M_X}\right)d\vec{K}$ and $P^T(\omega) = \int f_c^T(\vec{Q})F(\vec{Q})\delta\left(\hbar\omega - E^T_{1s} + \frac{\hbar^2 Q^2}{2m_e}\frac{M_X}{M_T}\right)d\vec{Q}$ for exciton and trion respectively. Their corresponding Boltzmann distribution are $f_c^T(\vec{Q}) = \frac{\hbar^2}{2\pi M_T k_B T}\exp\left(-\frac{\hbar^2 Q^2}{2M_T k_B T}\right)$ and $f_c^X(\vec{K}) = \frac{\hbar^2}{2\pi M_X k_B T}\exp\left(-\frac{\hbar^2 K^2}{2M_X k_B T}\right)$.

The trion oscillator strength given by $F(\vec{Q}) = \left|\int d\vec{\rho}_2 \psi_{1T}(0, \vec{\rho}_2)\exp\left(-\frac{i\vec{Q}\vec{\rho}_2 M_X}{M_T}\right)\right|^2$ where $\psi_{1T}(0, \vec{\rho}_2)$ is the trion eigenvector in the lowest state, the trion binding energy is $E_b^T = E^X_{1s} - E^T_{1s}$. We plot in fig.2, the exciton and trion PL emission calculated at 20K in (2a) WSe_2, WS_2 and (2b) $MoSe_2$, MoS_2.

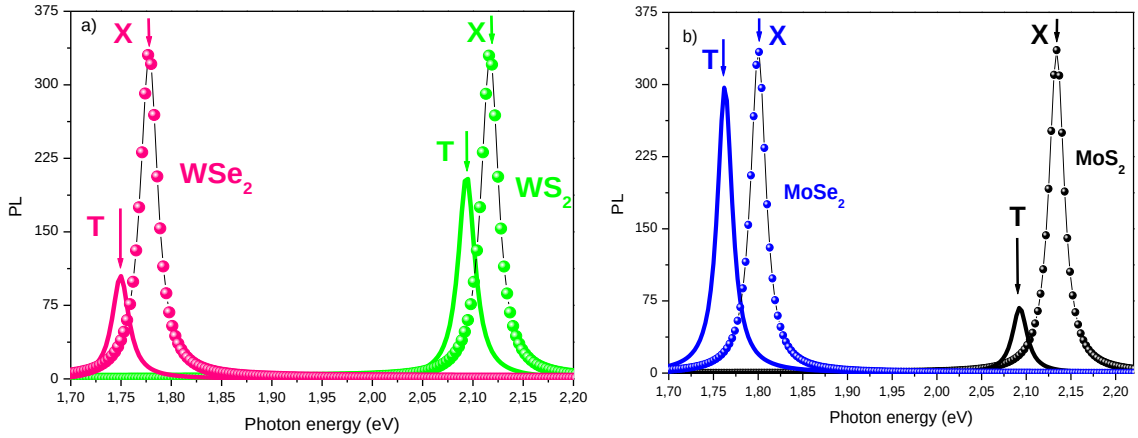

Fig. 2: PL spectrum of a monolayer TMDs on the SiO_2/Si substrate with ε_2 =3.9 and exposed to the air with $\varepsilon_1 = 1$. The emission peaks observed in the monolayer a) molybdenum and b) tungsten dichalcogenides are mainly attributed to the trion (T) emission whereas the relatively higher energies peaks, of each material, are assigned to the neutral exciton (X).

The calculated exciton and trion energies depend strongly on the diversity of the intrinsic parameters. The large trion binding energy observed in monolayer TMDs suggested the importance of trion. To the best of our knowledge, the exact values are still the subject of discussion, especially for monolayer WS_2, where the trion binding energy is still controversial. The trion binding energy is around 43 meV, 39 meV, 30meV and 25 meV respectively in monolayer MoS_2, $MoSe_2$, WSe_2 and WS_2.

4. Conclusion

To summarize, we have used a theoretical model taking into account the significantly reduced dielectric screening of coulomb interaction, to describe the exciton and trion in TMDs. Our calculations confirm theoretically that experimental data of the exciton and trion binding energies are of order of hundreds (excitons) and tenth (trions) meVs, which can be used in different technological applications at the room temperature regime.

References

[1] A. Splendiani, L. Sun, Y. Zhang, T. Li, J. Kim, C. Y. Chim, G. Galli, and F. Wang, "Emerging photoluminescence in monolayer MoS2, " *Nano Lett*., vol. 10, no. 4, pp.1271-1275, 2010.

[2] K. F. Mak and J. Shan, "Photonics and optoelectronics of 2D semiconductor transition metal dichalcogenides," *Nature Photonics*., vol. 10, pp. 216-226, 2016.

[3] B. Radisavljevic, A. Radenovic, J. Brivio, V. Giacometti, and A. Kis, "Single-layer MoS_2 transistors," *Nature Nanotechnology*., vol. 6, no. 10, pp. 147-150, 2011.

[4] B. Baugher, H. Churchill, Y. Yang, and P. Herrero, "Optoelectronic devices based on electrically tunable p–n diodes in a monolayer dichalcogenide," *Nature Nanotechnology*, vol. 9, pp. 262-267, 2014.

[5] F. K. Perkins, A. L. Friedman, E. Cobas, P. M. Campbell, G. G. Jernigan, and B. T. Jonker, "Chemical Vapor Sensing with Monolayer MoS_2," *Nano Lett*., vol. 13, no. 2, pp. 668-673, 2013.

[6] M. L. Tsai, S. H. Su, J. K. Chang, D. S. Tsai, C. H. Chen, C. I. Wu, L. J. Li, L. J. Chen, and J. H. He, "Monolayer MoS_2 heterojunction solar cells," *ACS Nano*., vol. 8, no. 8, pp. 8317-8322, 2014.

[7] Q. H. Wang, K. Kalantar-Zadeh, A. Kis, J. N. Coleman, and M. S. Strano, "Electronics and Optoelectronics of Two-Dimensional Transition Metal Dichalcogenides," *Nat. Nanotechnol*., vol. 7, no. 11, pp. 699-712, 2012.

[8] C. Zhang. A. Johnson, C.-L. Hsu, L.-J. Li, and C.-K, Shih, "Direct Imaging of Band Profile in Single Layer MoS_2 on Graphite: Quasiparticle Energy Gap, Metallic Edge States, and Edge Band Bending," *Nano Lett*., vol. 14, no. 5, pp. 2443-2447, 2014.

[9] D. K. Zhang, D. W. Kidd, and K. Varga, "Excited Biexcitons in Transition Metal Dichalcogenides," *Nano Lett*., vol. 15, no. 10, pp. 7002-7005, 2015.

[10] T. C. Berkelbach, M. S. Hybertsen, and D. R. Reichman, “Theory of Neutral and Charged Excitons in Monolayer Transition Metal Dichalcogenides,” *Phys. Rev.B* , vol. 88, no. 4, pp. 045318-045324, 2013.
[11] F. Cadiz, S. Tricard, M. Gay, D. Lagarde, G. Wang, C. Robert, P. Renucci, B. Urbaszek, and X. Marie, “Well separated trion and neutral excitons on superacid treated MoS_2 monolayer,” *Appl. Phys. Lett*., vol. 108, no. 10, pp. 1063, 2016.
[12] A. Singh, G. Moody, K. Tran, M. E. Scott, V. Overbeck, G. Berghäuser, J. Schaibley, E. J. Seifert, D. Pleskot, N. M. Gabor, J. Yan, D. G. Mandrus, M. Richter, E. Malic, X. Xu, and X. Li, “ Trion formation dynamics in monolayer transition metal dichalcogenides,” *Phys. Rev. B.*, vol. 93, no. 4, pp. 041401-041406, 2016.
[13] A. Chernikov, T. C. Berkelbach, H. M. Hill, A. Rigosi, Y. Li, O. B. Aslan, D. R. Reichman, M. S. Hybertsen, and T. F Heinz,, “Exciton binding energy and nonhydrogenic Rydberg series in monolayer WS_2,” *Phys. Rev. Lett*., vol. 113, no. 7, pp. 076802-076807, 2014.
[14] F. A. Rasmussen and K. S. Thygesen, “Computational 2D Materials Database: Electronic Structure of Transition-Metal Dichalcogenides and Oxides,” *Physical Chemistry.,* vol. 119, no. 10, pp. 13169-13183, 2015.
[15] Z. Ye, T. Cao, K. O’Brien, H. Zhu, X. Yin, Y. Wang, S. G. Louie, and X. Zhang, "Exciton Binding Energy of Monolayer WS_2," *Sci. Rep*., vol. 5, no. 9218, 2015.
[16] A. V. Stier, K. M. McCreary, B. T. Jonker, J. Kono, and S. A. Crooker, “Exciton diamagnetic shifts and valley Zeeman effects in monolayer WS_2 and MoS_2 to 65 Tesla,” *Nat. Nanotechnol*., vol. 7, no. 10643, 2016.